The object of this study is lightweight concrete wall structures treated with various types of conventional plasters. The problem addressed in the paper is to determine the effectiveness of different types of plastering to protect walls from the effects of high temperatures and improve the fire resistance of structures.

The samples of one series were fabricated by plastering the aerated concrete wall with a cement-lime plaster while the samples of the other series were plastered with vermiculite-perlite plaster. Samples of the third series were made without plastering (control series). In accordance with the research program, the distribution of temperatures under fire load was determined for all series.

Studies have shown that wall structures plastered with verliculite-perlite mortar demonstrated 3.8 times better thermal insulation characteristics compared to plastering with cement-lime mortar. The fire protection effect of plastering (compared to non-plastered samples) for vermiculite-perlite solution was 6.3 times, and for cement-lime – 1.6. Adhesion failure was observed in cement-lime plaster under high temperatures, highlighting the need for additional fixing when applied to lightweight concrete walls. Theoretical analysis of the results revealed a discrepancy of up to 19 % with the experimental findings.

The high thermal insulation properties of vermiculite-perlite plasters in comparison with cement-lime plasters are well known. A distinctive feature of this study is the quantitative determination of temperature distribution for the investigated plasters under conditions approximating real fire exposure.

The findings of this research can be applied to the design of buildings and structures requiring enhanced fire resistance for wall systems

Keywords: *fire resistance, thermal insulation capacity, enclosing structures, fire, plaster, temperature distribution*

UDC 624.012.46
DOI: 10.15587/1729-4061.2024.317342

DETERMINING THE IMPACT OF PLASTERING MATERIALS ON TEMPERATURE DISTRIBUTION IN LIGHTWEIGHT CONCRETE ENCLOSURE STRUCTURES EXPOSED TO FIRE

Serhiy Bula
PhD, Associate Professor
Department of Building Constructions and Bridges
Institute of Civil Engineering and Building Systems
Lviv Polytechnic National University
Karpinskoho str., 6, Lviv, Ukraine, 79013
E-mail: serhii.s.bula@lpnu.ua

Received 20.09.2024
Received in revised form 18.11.2024
Accepted 28.11.2024
Published 27.12.2024

How to Cite: *Bula, S. (2024). Determining the impact of plastering materials on temperature distribution in lightweight concrete enclosure structures exposed to fire. Eastern-European Journal of Enterprise Technologies, 6 (10 (132)), 46–54. https://doi.org/10.15587/1729-4061.2024.317342*

1. Introduction

Ensuring the fire resistance of building structures is a critically important task in modern construction as the safety of people and the preservation of buildings in the event of a fire largely depend on it. The increase in requirements for fire resistance of structures is driven not only by the number of fires in residential buildings [1] but also to current fire safety regulations, which require reliable protection of load-bearing elements of structures from exposure to high temperatures [2].

Current scientific research is focused on finding effective solutions for passive fire protection, in particular the use of materials capable of increasing thermal insulation properties. The use of specialized fire-resistant materials, such as paints, varnishes, and special cladding panels, provides a high level of protection. However, these materials are often expensive and not always available. Therefore, tackling the search for more affordable materials, in particular, the use of conventional plastering solutions, is a promising direction that could improve the thermal insulation characteristics and increase the fire resistance of wall structures.

Research on the effectiveness of conventional plasters in passive fire protection is essential for practical applications, as it allows for evaluating the potential of commonly used materials in ensuring fire safety. Furthermore, experimental studies under real fire exposure conditions are necessary to refine theoretical models and accurately predict temperature distribution.

2. Literature review and problem statement

To calculate the fire resistance of masonry structures in accordance with current standards, it is essential to determine the temperature distribution across the wall's cross-section [3]. Clearly, the presence of finishing layers, such as plasters, influences this distribution. As a result, the performance of plasters under high-temperature exposure has been the focus of numerous scientific studies.

Study [4] analyzed the performance of perlite plaster (EPAP) compared to conventional plaster (NAP) at high temperatures. Various plaster thicknesses were studied under local fire exposure (gas burner) lasting 180 min and a constant temperature of 900 °C. The results showed that the temperature on the reverse side of the EPAP plates was half as low (≈105 °C) as that of the NAP plates (≈225 °C). Quantitative backside temperatures were obtained, indicating better fire resistance of EPAP compared to NAP. However, the research was directly related to the stucco material, which was tested separately from the wall structure. Therefore, the issue of temperature distribution in the general wall structure remained unresolved.

Copyright © 2024, Authors. This is an open access article under the Creative Commons CC BY license

In work [5], the performance of self-compacting heavy concrete (SCC) with various energy-efficient additions to cement under the influence of high temperatures was analyzed. In particular, residual strength and impact resistance after a fire were investigated. The research program also included tests in an electric furnace of concrete cube samples covered with cement-perlite plaster (CPP) with a thickness of 20 mm. The temperature regime in the furnace corresponded to the standard temperature curve and lasted 120 minutes. In the course of research, the thermal insulation effect of the CPP solution was recorded. At a temperature on the surface of ≈920 °C (60 min of heating), the temperature in the thickness of the plaster was 492 °C and 205 °C in the thickness of the sample. For unprotected samples, the temperature in the thickness of the sample reached 613 °C. The advantage of the study is the test in the "plaster-material" system. However, the issue of thermal insulation effect for structures made of light concrete remained unexplored in the work. Small experimental samples are also a limitation.

Study [6] examines the problems associated with the fire protection of structural concrete in the event of a fire. To solve these problems, the possibility of using light plasters on high-strength concrete (HSC) is being investigated. Three types of insulating plasters have been designed: sand plaster (SP), gypsum with the addition of perlite (GPP), and gypsum with the addition of mineral wool fibers (GMP). Compressive strength, adhesion, and shear strength after exposure to standard fire temperature under different fire extinguishing conditions (air and water) were investigated. The investigated plasters were applied with a thickness of 15 mm on concrete cubes on prisms and were examined for temperature effects in an electric furnace according to a standard temperature curve. Between the results of the residual strength and adhesion tests, the temperature distribution under the surface of the plaster was obtained. In particular, for 60 min of heating to ≈920 °C, the temperature under the plaster was ≈400 °C, ≈325 °C, and ≈180 °C for the SP, GPP, and GMP series, respectively. As in the previous study, experiments were not conducted on wall structures with plasterboard.

Paper [7] investigated the effectiveness of plasters for passive fire protection of steel structures. The tests carried out included small-sized coated steel plates and short steel columns, in which the thermal performance at high temperatures was evaluated. Solutions based on Portland cement, vermiculite, and polypropylene fibers (DCM), gypsum and perlite (DGMP), gypsum and vermiculite (DGMV), recycled cement, perlite and vermiculite (DRCM) and conventional Portland cement (CM) were investigated. The thickness of the plaster was 10 mm, the heating temperature was 900 °C. The samples were heated gradually (60 min) until they reached the maximum temperature and kept at this temperature for 120 min. For 60 minutes of heating, the temperature of the inner surface of the plaster was ≈400 °C for all studied types of plaster on small-sized models. Valuable results were obtained on small-sized and medium-sized models regarding the protective properties of plasters. However, the study of plasters took place on steel structures that have different physical and mechanical characteristics and thermal inertia than walls.

Work [8] describes changes in the properties of concrete during a fire and its protection with the help of heat-insulating plaster. The authors established that fire-resistant plaster with low thermal conductivity could slow down the rise in temperature on the concrete surface. Under the influence of a flame with a temperature of more than 800 °C for 30 min, the temperature under the plaster did not exceed 120 °C, which indicates the effectiveness of the protective layer. The addition of aluminosilicate microspheres to the plaster contributes to the formation of a heat-protective layer, which reduces heat transfer and increases the resistance of concrete to mechanical influences. However, lightweight autoclaved concrete, as a base material for the plaster, was not studied by the authors.

Studies [9] describe a number of fire studies on wall samples. The fire resistance of full-size wall structures made of stone and brick in fire furnaces was investigated. The studies concerned structures of various types and contain a lot of valuable information about their performance during fire exposure, but the samples were studied without applied finishing layers.

Paper [10] discusses traditional surface finishing materials such as clay and lime plaster used on wooden walls and ceilings of historic buildings. The paper examines the thermal properties of historical plasters depending on the temperature by means of the study of materials in the furnace under standard conditions of fire exposure. However, the authors did not cover the comparative study of modern clay and lime materials.

In study [11], the fire protection effect of covering heat-insulating boards with plaster was investigated. Protection was investigated for expanded polystyrene (EPS), extruded polystyrene (XPS), and mineral wool (RW) boards. Plaster on a cement-sand base with a thickness of 2, 4, 6, and 8 mm on small-sized elements was studied. The fire load was applied locally using a torch with a maximum duration of 25 minutes. A significant decrease in the strength and adhesion of the studied plaster by 58 % at a temperature of 600 °C was recorded. Wall structures were not included in the research program, so this issue remained unexamined.

Cladding of building structures with dry gypsum plaster in the form of plates is also widely used. In study [12], structures decorated with a layer of plasterboard with a thickness of 12 mm were compared. The temperature distribution for 40 min of heating was 510 °C and 280 °C on the surface and 220 °C and 130 °C and at a depth of 5 mm for the unprotected and protected element. In [13], the fire protection of a wooden frame with plasterboard was investigated. The use of fire protection from gypsum boards delays the charring process of wood by approximately 35 %. Researchers of such systems confirm a significant fire-protective effect; however, the heat-protective effect of lining structural wall materials has not been investigated.

The review of available literature demonstrated that the issue of temperature distribution in the "plaster-wall structure" system remains insufficiently elucidated. Most studies assume heavy concrete, steel, and wood as the basis for plaster. There are also papers that focus only on the study of the plaster material without interaction with the base. Small-scale samples and electric furnaces are often accepted by researchers as a test environment, which is due to the costs of conducting large-scale studies.

Therefore, it is expedient to study the effect of plastering on the temperature distribution in wall structures made of autoclaved aerated concrete using medium-sized wall samples exposed to parametric fire conditions.

3. The aim and objectives of the study

The purpose of our study is to determine the effect of plaster materials on the temperature distribution in auto-

claved aerated concrete (AAC) enclosing structures under conditions resembling a real fire. The results will aid in accounting for this effect when calculating the fire resistance of such structures during design.

To achieve this goal, the following tasks need to be resolved:

– experimentally determine the temperature distribution in the studied structures under fire load;

– perform numerical modeling to evaluate the convergence with experimental results.

4. The study materials and methods

4. 1. The object and hypothesis of the study

The object of this study is the influence of the plaster material on the temperature distribution in the aerated concrete block walls under fire temperature load.

The principal hypothesis assumes that plaster material affects temperature distribution, and accounting for its real performance at high temperatures could help optimize wall thickness based on fire resistance criteria.

During the research, it was ensured that thermocouples in individual series were positioned at enough distances to eliminate mutual heat transfer influence between different sample series. To simplify the design and simulate more extreme conditions, grids were not used for plaster installation - fastening was achieved solely through adhesion. The simplification of the calculation model involved neglecting moisture transfer and material density changes during the heating process.

4. 2. Preparation of samples

The investigated wall structure was constructed using AAC blocks by TM Aeroc® (Ukraine) with a density of D500 and dimensions of 200×200×600 mm. Two types of plaster and control samples without coating were examined.

One face of the wall structure was divided into three sections: one section was plastered with a cement-lime solution (CLP series), and another with a perlite-vermiculite solution (PVP series). Both plasters were applied in strips 20 cm wide and 20 mm thick. The central section was left uncoated, serving as the control sample (CTRL series). The placement of the plastering areas on the same wall face ensured a uniform temperature regime on the heated surface. The AAC blocks were assembled using TM Polimin PB-55® (Ukraine) adhesive mixture. The moisture content of the materials was measured with a Testo® 606–1 electronic moisture meter (PRC).

Samples of the CLP series were plastered with a cement-lime solution by TM Ferozit® 220 (Ukraine) [14], while the PVP series was coated with perlite-vermiculite plaster by TM Bauwer Standard® [15].

The preparation of samples was performed according to the technological guidelines provided by the manufacturers [14, 15]. The base surface was treated in accordance with the requirements of DSTU-NB V.2.6-212:2016 and DSTU-NB A.3.1-23:2013.

The surfaces were mechanically cleaned of dust and adhesive residues, and the aerated concrete blocks were thoroughly moistened. For the CLP series, the surface was treated with Ferozit® 17 Betoncontact adhesive paint, while for the PVP series, it was treated with Bauwer Basis® cement spray.

Both plaster solutions were prepared from dry construction mixtures by mixing with water according to the manufacturer's instructions. To ensure proper hydration, the plaster surfaces were moistened for the first three days. Testing was conducted no earlier than 28 days after plaster application.

4. 3. Research methods

Testing of experimental samples was carried out at the laboratory of fire safety (Fig. 1, *a*, *b*), Lviv Polytechnic National University. The test samples were tested according to the guidelines from [16], but the temperature regime was changed from standard to parametric, since direct determination of the fire resistance limit was not the goal of the study.

Fig. 1 shows a furnace [17] for fire tests of building structures and thermophysical tests of materials. The structure is a box made of fire-resistant materials, which consists of walls, a removable partition, and a cover. Holes for fuel and measuring equipment are made in the longitudinal walls. The overall dimensions of the furnace for testing are 4100×1800 mm, but for these tests a section of the chamber measuring 1800×1300×600 mm was used.

Diesel fuel is used as fuel for the burner in the furnace. From the tank, the fuel enters the fuel pump through the filter, which creates the pressure necessary for spraying.

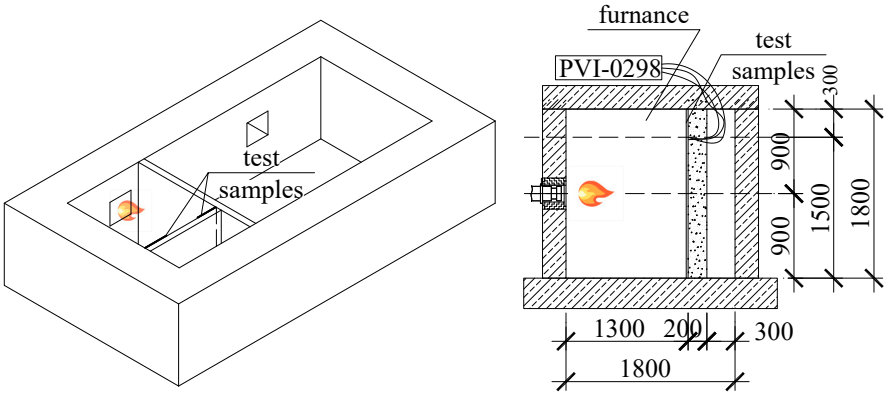

Fig. 1. General view of the furnace: *a* — general view of the experimental installation; *b* — the scheme of setting samples in the fire chamber

When leaving the nozzle, the fuel enters the air stream, which is swirled by the swirler. The resulting fuel-air mixture is ignited by a spark discharge and burns, thus creating the necessary temperature load in the fire chamber. The temperature was measured using chromel-alumel thermocouples. The arrangement scheme is shown in Fig. 2.

In addition to thermocouples embedded within the sample, the temperature regime in the chamber was monitored at a distance of 2 cm from the heated sample surface. Fig. 3 shows the installation before and during the tests. To ensure the reliability and validity of the results, two iterations of research were conducted (average results are given below).

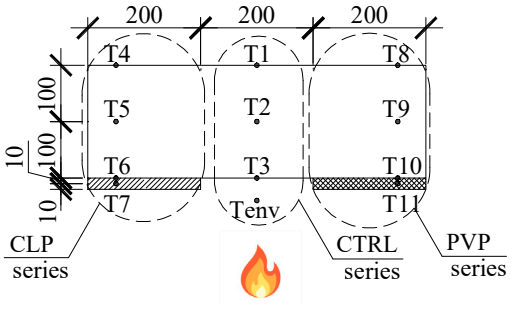

Fig. 2. Schematic arrangement of thermocouples in samples

a

b

Fig. 3. Conducting tests: *a* — temperature measurement during tests; *b* — inspection of the bench before the test

The signal from the thermocouples was processed using two PVI-0298 measuring transducers (Ukraine), which transmit information to a personal computer. Before the start of the experiment, calibration procedures of thermocouples and measuring transducers were performed to ensure high accuracy of temperature measurements. The time to read information from one thermocouple was less than one second. The accuracy of the measurements was 1 °C. The temperature load on the test samples lasted 60 minutes. The initial temperature of the samples was 10 °C, the air humidity was 56 %. The maximum temperature of the environment in the furnace on the heating side reached 770 °C. The heating temperature regime was close to, but lower than, the standard heating curve according to ISO 834 [18] and corresponded to the parametric temperature curve. Parametric temperature regimes better reflect real scenarios of fires in premises taking into account ventilation openings, mass of combustible materials, and other characteristics of the premises. After completion of heating, the samples were cooled naturally.

5. Results of investigating plastering materials under temperature stress

5. 1. Experimental determination of temperature distribution in sample cross sections

Based on the data acquired at the control points, temperature-time dependency plots were constructed for all studied series (Fig. 4, 5). The temperature readings after 60 minutes of heating are summarized below. As could be seen from the plots in Fig. 4, *a*, on the reverse, unheated side of the wall, the temperature rose slightly by 5 °C relative to the initial temperature for samples without plaster. Temperature indicators for both series of plastered samples remained unchanged. In the middle of the cross-section of the aerated concrete block (Fig. 4, *b*), the distribution plot shows higher temperature values: 74 °C for the control samples and 55 °C and 41 °C for the CLP and PVP series, respectively. A similar trend was observed at the interface between the plaster and the block. The recorded temperatures were 619 °C for the CTRL series, 378 °C for the CLP series, and 98 °C for the PVP series (Fig. 5, *a*).

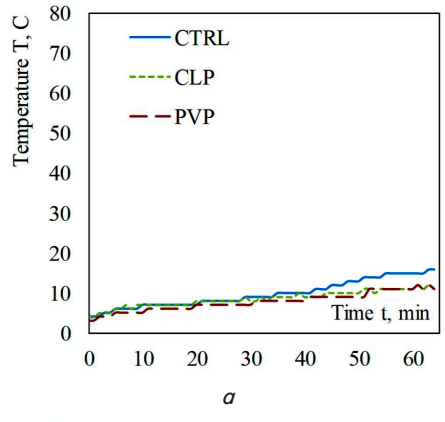

a

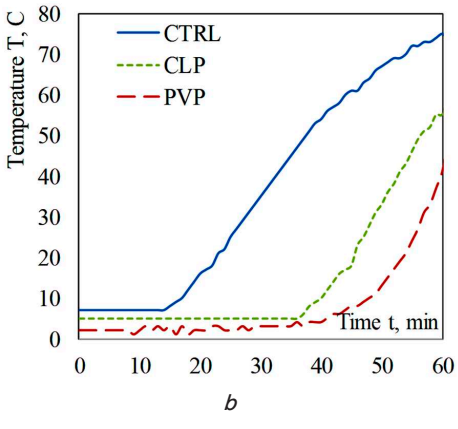

b

Fig. 4. Temperature distribution in the thickness of the samples: *a* — on the unheated surface (thermocouple T4, T1, T8); *b* — on the middle surface (thermocouple T5, T2, T9)

In the middle of the plaster thickness (Fig. 5, *b*), the maximum heating of CLP series samples was 541 °C for CLP series samples and 286 °C for PVP samples. The control samples did not have plastering solutions, and the temperature corresponded to the temperature of the environment T_{env}=770 °C.

Analysis of temperature distribution plots in the thin layer (Fig. 5, *a*, *b*) clearly reveals horizontal sections (marked by arrows). They indicate the slowing down of heating due to heat consumption for the evaporation of pore water at

a temperature of ~100 °C. Therefore, after evaporation of chemically unbound water after 20 min the heating of the material (PVP series) returns to a more intensive mode. As could be seen, in PVP samples, these areas are significantly longer due to the larger number of pores due to the structure of the clay material. In total, this slowdown was 60 min for the PVP series and 10 min for the CLP series.

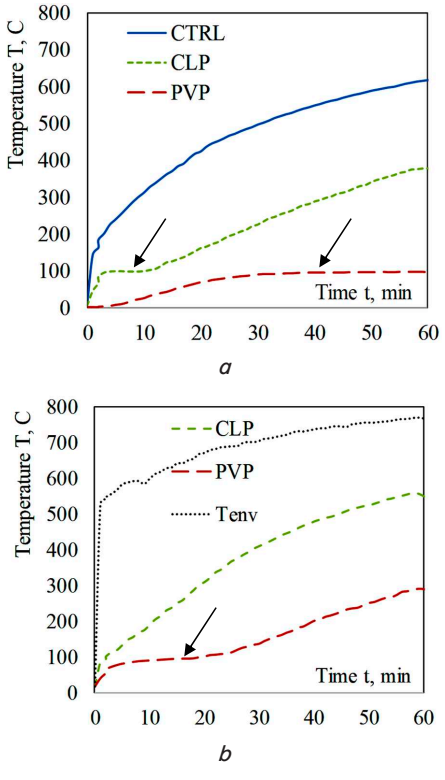

Fig. 5. Temperature distribution under the surface of the plaster at a distance: *a* — 20 mm (thermocouple T6, T3, T10); *b* — 10 mm (thermocouple T7, T11)

Fig. 6, 7 show the distribution of temperatures in the cross section of the studied samples at different stages of heating (the plane of the plaster is shown in gray, and the plane of the wall block is shown in white). The difference between the temperature of the fire medium and the surface temperature of the block under the plaster for 15 minutes of heating (Fig. 6, *a*) is Δ_{CTRL}=272 °C, Δ_{CLP}=517 °C, Δ_{PVP}=593 °C. With the duration of the temperature effect on the plaster, the temperature differences change. Thus, over 60 minutes of heating (Fig. 7, *b*), these indicators were Δ_{CTRL}=153 °C, Δ_{CLP}=392 °C, Δ_{PVP}=673 °C. As could be seen from the comparison of the plots at the end and at the beginning of heating, only for samples of the PVP series, the difference does not decrease, which indicates the preservation of the thermal insulation properties of the plaster.

After the fire exposure, the test samples were examined, and a visual comparison of the plaster condition was conducted (Fig. 8).

Shortly after the temperature exposure ended, a significant portion of the CLP series plaster detached completely and fell to the bottom of the fire chamber. Surface chips and craters also developed. For the PVP series, structural changes caused by dehydration led to increased surface roughness. Microcracks were observed on both types of plaster.

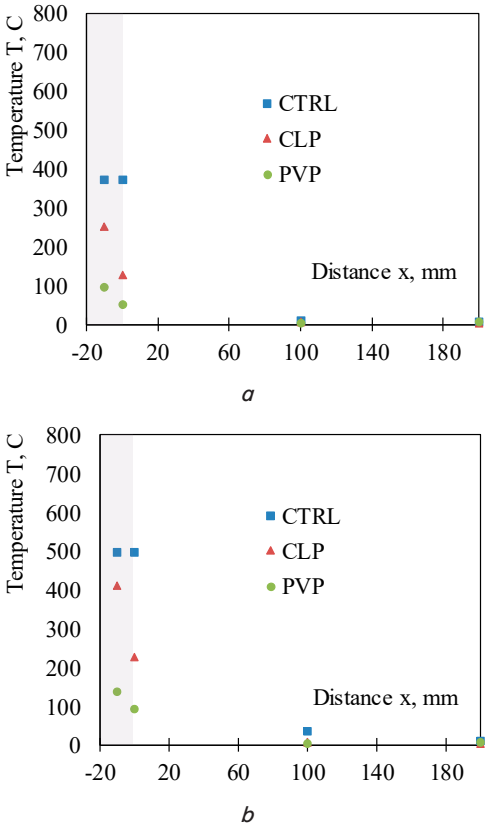

Fig. 6. Temperature distribution in the thickness of the samples: *a* — minute 15 of heating (T_{env}=642 °C); *b* — minute 30 of heating (T_{env}=705 °C)

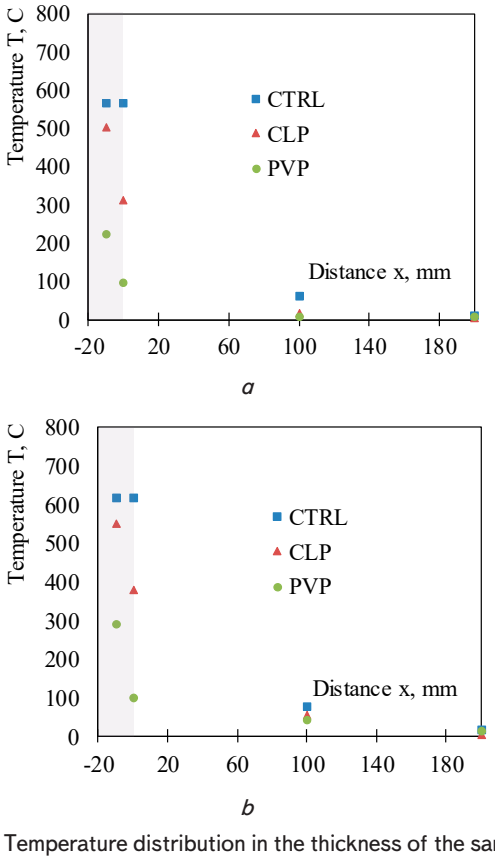

Fig. 7. Temperature distribution in the thickness of the samples: *a* — minute 45 of heating (T_{env}=745 °C); *b* — minute 60 of heating (T_{env}=770 °C)

Fig. 8. Peeling of CLP series plaster during the curing of the structure

5. 2. Numerical modeling of temperature distribution in sample cross sections

To determine the temperature distribution by calculation, the Fourier law (1) was used for a two-dimensional problem with a non-linear temperature regime and non-linear thermophysical characteristics of materials [19]:

$$\frac{\partial}{\partial x}\left(\lambda_x \frac{\partial T}{\partial x}\right)+\frac{\partial}{\partial y}\left(\lambda_y \frac{\partial T}{\partial y}\right)=-q(T)-c(T)\rho\frac{\partial T}{\partial t}, \quad (1)$$

where T is temperature, t is time, $\lambda(T)$ is specific thermal conductivity, ρ is density, $c(T)$ is specific heat capacity, $q(T)$ is specific power of heat sources.

The initial (2) and boundary conditions for the convective (3) and radiative (4) components of the heat flow at the faces of the elements were also specified [2].

Initial conditions:

$$T(x,y,0)=T_0(x,y,), \quad (2)$$

boundary conditions:

$$F_n=\alpha(T-T_0), \quad (3)$$

$$F_n=k_{sb}\beta\left(T^4-T_0^4\right), \quad (4)$$

where α is the convection heat transfer coefficient (W/(m^{2}K);

T is the temperature of the external environment (K);

T_0 is the initial temperature (K);

k_{sb} is the Stefan-Boltzmann constant (W/(m^{2}K^4);

β is the emissivity coefficient of the surface.

The QuickField® software package [20] was used to perform the calculations. This is a software suite for calculating problems of thermodynamics, electromagnetism, and stress analysis. Owing to the convenient and intuitive interface (Fig. 9), the parameters of the geometry, material properties, boundary conditions of the heat flow on the surfaces were set, and the calculation was performed using the finite element method.

For correct numerical modeling, it is necessary to have information about the thermophysical characteristics of materials at high temperatures. However, manufacturers of conventional plasters do not provide such indicators, therefore, values based on temperature studies of similar materials were adopted (Table 1). Intermediate values were taken by interpolation. To simplify calculations, it is assumed that the density of materials does not change during heating.

The coefficients for convection and radiation component were used to define the boundary conditions for heat transfer on the element faces (Table 2). The exposed temperature load function was based on actual measurements obtained from the furnace data.

As a result, the distribution of temperature fields in the samples of different series over the entire heating time was obtained. Fig. 10 shows temperature distribution in the cross section at the 60th minute of heating.

Table 1

Calculated thermophysical characteristics of materials [3, 14, 15, 22, 23]

Series	Density ρ, kg/m^3	Thermal conductivity λ, W/m K		Heat capacity C, J/kg K		Source
		20 °C	500 °C	20 °C	500 °C	
CLP series	1600 [14]	0.7	0.3	900	1350	[23]
PVP series	330 [15]	0.08	0.25	800	1200	[22]
Aerated concrete	500	Fig. D1(d) annex D.		Fig. D1(d) annex D.		[3]

Table 2

Boundary conditions adopted in the calculation [2, 24]

Parameter name, symbol	Measurement unit	Value	Source
Convection heat transfer coefficient for the surface to be heated, α_c	W/m^{2}K	25	[2]
Convection heat transfer coefficient for a surface that is not subject to heat, α_c	W/m^{2}K	9	[2]
Emissivity coefficient, β	Dimensionless	0.91	[24]
Initial surface temperature, T_0	K	Experimental data	
Exposed temperature, T	K		

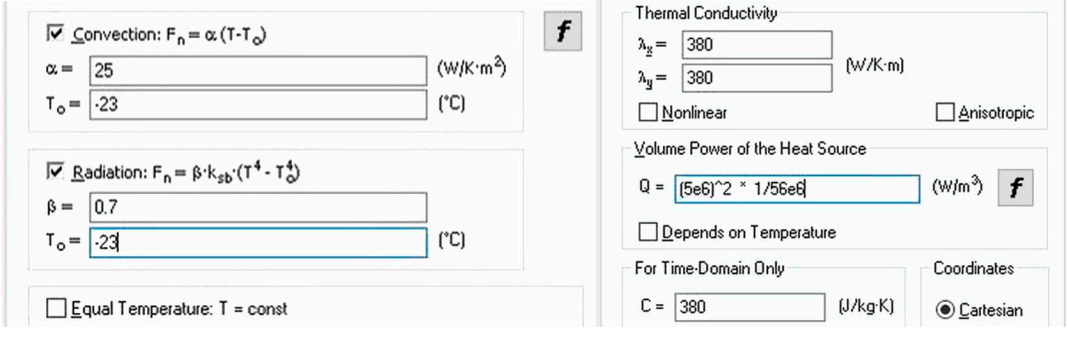

Fig. 9. Interface of the QuickField software package [21]

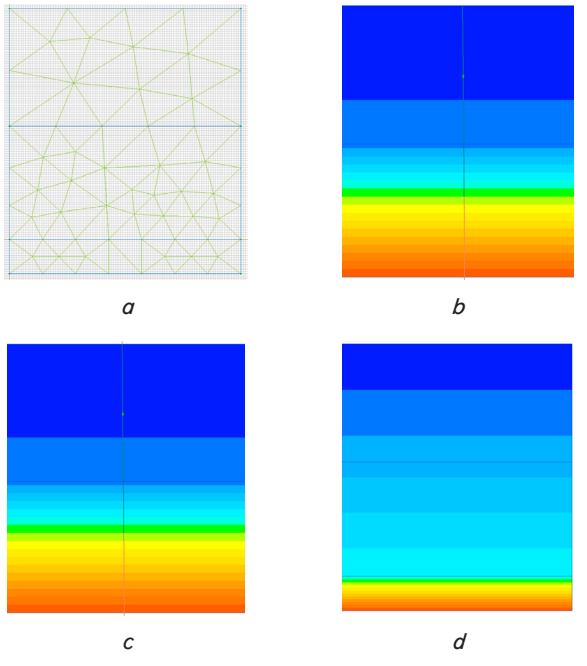

Fig. 10. Results of the numerical simulation of temperature distribution: *a* — grid of finite elements; *b* — for samples of the CTRL series (60 min); *c* — for samples of the CLP series (60 min); *d* — for samples of the PVP series (60 min)

In general, the difference in results ranged from 5 % to 19 %. The largest discrepancy compared to the experimental results occurred when the temperature approached ~100 °C, as the software package does not account for moisture transfer.

6. Discussion of experimental research results

The investigated structure was tested as a self-supporting, enclosing partition that does not bear external loads. Accordingly, the fire resistance of the structure is assessed based on its loss of heat-insulating ability. Under the standard heating regime, the limit state for this criterion is defined as one of two conditions. An increase in the average temperature on the unheated surface of the sample exceeding the initial average temperature by 140 °C. Or an increase in temperature at any arbitrary point on the unheated surface exceeding the initial temperature at that point by 180 °C [25]. Note that this limit state was not reached for any of the studied structures under the influence of the experimental temperature load. The temperature on the unheated surface changed within 5 °C only in samples without plastering (Fig. 4, *a*). From the analysis of temperature distribution plots (Fig. 4, *a*, *b*), it could be seen that for walls made of aerated concrete 200 mm thick, the effect of plastering 20 mm is very insignificant.

At the middle point of the wall block, the effect of plastering becomes more noticeable and shows 25 % (CLP) and 45 % (PVP) lower temperature values compared to the control samples (Fig. 4, *b*).

Extending the analysis of test results, it could be noted that the intensity of evaporation of pore water in the material significantly affects the subsequent thermal conductivity of the structure. PVP samples, because of the greater porosity due to the perlite-vermiculite composition, show a longer period of water evaporation, which contributes to better thermal insulation. This slowdown is also related to the fact that the evaporation of pore water is a phase transition that absorbs a large amount of thermal energy, delaying further heating. At the same time, CLP samples have a smaller number of pores, which causes faster water evaporation and correspondingly less efficiency in heat retention.

The influence of the heat-insulating ability of the plaster is clearly visible in Fig. 5, *a*, where at the end of heating, the difference compared to the CTRL series was 39 % (CLP) and 16 % (PVP). The same trend is observed for the plane in the middle of the plaster: 30 % for the CLP series and 62 % for the PVP series (Fig. 5, *b*).

Fig. 6, 7 show the distribution of temperatures in the thickness of the structure at different stages of heating. They clearly demonstrate the heat-insulating effect of finishing plasters. For example, on minute 60 of heating, the surface of an aerated concrete block without decoration is 617 °C, on the other hand, the temperature of the surface under the plaster of the CLP series is 378 °C, and the PVP series is 97 °C. This indicates a significant heat-insulating effect of even conventional plasters under fire conditions. Accordingly, the temperature of the face of the wall as an enclosing structure in this case has a protective effect due to the plaster at Δ_{CLP}=239 °C, Δ_{PVP}=520 °C in comparison with undecorated samples.

The destruction of the CLP series plaster shows the need for additional measures for fixing the plaster to the wall. Taking into account the negative effect of high temperatures on the adhesion of plasters, it is necessary to ensure reliable fastening of plasters to the walls. This could be achieved through the correct selection of plastering solutions in relation to the material of the wall and with the help of the arrangement of steel reinforcing grids for solutions, notches on the surface of the blocks, additional adhesive solutions, etc. The destruction of the PVP series plaster didn't happen at all. This is likely due to the lower pore water pressure in the more porous material (compared to the PLC series). Also, the plaster of this series has a similar porous structure to the aerated concrete block, which reduces temperature stresses at the contact of the materials.

In contrast to previous studies [4–11], in which attention was paid to specialized plasters, the current study considered plasters that are widely represented in the modern construction market and are used on a mass level. This approach ensures a greater practical value of the results because the investigated plasters were tested on full-size models of light autoclaved concrete walls, which better reproduces the real conditions of fire load. The results of the experiments showed that conventional plasters have the potential to increase the thermal insulation capacity of the enclosing structures, which makes it possible to more accurately determine their fire resistance limit according to the thermal insulation criterion (*I*).

The practical significance of this research relates to determining the effectiveness of conventional plasters, which are widely used in modern construction, to improve the fire resistance of lightweight concrete wall structures. Applying the research results could contribute to optimizing the design of building structures. The proposed methodologies of analysis and experimental evaluation could be used to devise recommendations for the application of plasters in construction practice.

The findings may have limitations in determining the actual fire resistance characteristics due to the unpredict-

ability of plaster adhesion properties during a fire. Accurate consideration of their thermal properties in calculations is only possible if reliable fastening of the plaster to the wall structures is ensured. Additionally, numerical modeling may yield less precise predictions because of insufficient data on the changes in the thermophysical properties of plasters at high temperatures, which constrains the accuracy of the calculations.

A significant drawback of the applied experimental approach is the high cost of conducting fire tests on medium-sized samples in a fire chamber, which may restrict the frequency of such studies. Nevertheless, these experiments are essential for obtaining reliable results that address existing gaps in the research on the fire resistance of plasters. Future research in this area could focus on evaluating other types of plaster and structural materials, as well as optimizing experimental methods to reduce testing costs and labor intensity.

7. Conclusions

1. Experimental studies have demonstrated that the application of plaster reduces the temperature at the contact interface between the plaster and the autoclaved aerated concrete block compared to non-plastered samples. For cement-lime plaster (CLP), the contact temperature was reduced by Δ_{CLP}=239 °C (a 1.6-fold reduction), and for perlite-vermiculite plaster (PVP) by Δ_{PVP}=520 °C (a 6.3-fold reduction). Perlite-vermiculite plaster proved to be 3.8 times more effective than cement-lime plaster in terms of fire protection. This result can be attributed to the superior thermal insulation properties of PVP, owing to its high content of perlite and vermiculite, which exhibit low thermal conductivity. After one hour of fire exposure, the contact temperature was 378 °C for CLP and only 98 °C for PVP, highlighting its significant protective potential under elevated temperature conditions.

2. Numerical simulation using the finite element method has confirmed the viability of this approach for estimating temperature distribution in lightweight concrete structures with plaster. The discrepancy between the numerical and experimental data did not exceed 19%, which is within an acceptable range for predicting structural performance under high-temperature conditions. To further improve the agreement between numerical modeling results and experimental data, it is necessary to account for changes in the thermophysical properties of the plaster during heating, as well as the parameters of temperature exposure.

Conflicts of interest

The author declares that he has no conflicts of interest in relation to the current study, including financial, personal, authorship, or any other, that could affect the study, as well as the results reported in this paper.

Funding

The study was conducted without financial support.

Data availability

All data are available, either in numerical or graphical form, in the main text of the manuscript.

Use of artificial intelligence

The author confirms that he did not use artificial intelligence technologies when creating the current work.

Acknowledgments

The author expresses his gratitude to the technical staff of the fire safety laboratory for their help in conducting experimental tests.

References

1. Analitychna dovidka pro pozhezhi ta yikh naslidky v Ukraini za 12 misiatsiv 2023 roku (2024). Kyiv. Available at: https://idundcz.dsns.gov.ua/upload/2/0/1/8/2/6/2/analitychna-dovidka-pro-pojeji-122023.pdf
2. EN 1991-1-2: Eurocode 1: Actions on structures - Part 1-2: General actions - Actions on structures exposed to fire. Available at: https://www.phd.eng.br/wp-content/uploads/2015/12/en.1991.1.2.2002.pdf
3. EN 1996-1-2: Eurocode 6: Design of masonry structures - Part 1-2: General rules - Structural fire design. Available at: https://www.phd.eng.br/wp-content/uploads/2015/02/en.1996.1.2.2005.pdf
4. Ulusu, İ., Kurnuç Seyhan, A. (2023). Effect of Expanded Perlite Aggregate Plaster on the Behavior of High-Temperature Reinforced Concrete Structures. Buildings, 13 (2), 384. https://doi.org/10.3390/buildings13020384
5. Mathews, M. E., Kiran, T., Nammalvar, A., Andrushia, A. D., Alengaram, U. J. (2023). Efficacy of Fire Protection Techniques on Impact Resistance of Self-Compacting Concrete. Buildings, 13 (6), 1487. https://doi.org/10.3390/buildings13061487
6. Kiran, T., Yadav, S. K., N, A., Mathews, M. E., Andrushia, D., lubloy, E., Kodur, V. (2022). Performance evaluation of lightweight insulating plaster for enhancing the fire endurance of high strength structural concrete. Journal of Building Engineering, 57, 104902. https://doi.org/10.1016/j.jobe.2022.104902
7. Caetano, H., Laím, L., Santiago, A., Durães, L., Shahbazian, A. (2022). Development of Passive Fire Protection Mortars. Applied Sciences, 12 (4), 2093. https://doi.org/10.3390/app12042093
8. Tsapko, Y., Bondarenko, O. P., Tsapko, O., Sukhanevych, M. (2024). Justification of the Efficiency of Application of Plaster for Fire Protection of Concrete Structures. Defect and Diffusion Forum, 437, 69–78. https://doi.org/10.4028/p-hdz0vg
9. Daware, A., Naser, M. Z. (2021). Fire performance of masonry under various testing methods. Construction and Building Materials, 289, 123183. https://doi.org/10.1016/j.conbuildmat.2021.123183

10. Johanna, L., Judith, K., Alar, J., Birgit, M., Siim, P. (2019). Material properties of clay and lime plaster for structural fire design. Fire and Materials, 45 (3), 355–365. https://doi.org/10.1002/fam.2798
11. Uygunoğlu, T., Özgüven, S., Çalış, M. (2016). Effect of plaster thickness on performance of external thermal insulation cladding systems (ETICS) in buildings. Construction and Building Materials, 122, 496–504. https://doi.org/10.1016/j.conbuildmat.2016.06.128
12. Demchyna, B. H., Pelekh, A. B., Oleksyn, H. M., Surmai, M. I. (2009). Povedinka doshchatokleienykh kolon za mistsevoho vplyvu vysokoi temperatury. Visnyk NULP: Teoriya i praktyka budivnytstva, 655, 71–74. Available at: https://ena.lpnu.ua:8443/server/api/core/bitstreams/723343d9-c33b-4ab0-808f-d6889eaea74a/content
13. Pelekh, A. B., Demchyna, B. H., Shnal, T. M., Bula, S. S., Krochak, O. V. (2008). Naturni vyprobuvannia konstruktsiyi derevianoi ramy na vohnestiykist v umovakh realnoi pozhezhi. Visnyk NULP: Teoriia i praktyka budivnytstva, 6275, 167–172. Available at: https://vlp.com.ua/files/34_17.pdf
14. Ferozit 220. Available at: https://ferozit.ua/wp-content/uploads/2017/06/TK-F-220-2024.pdf
15. Teploizoliatsiyna sumish Bauwer Standard. Available at: https://bauwer.ua/images/products/pdf/Standard.pdf
16. EN 1364-1:2015. Fire resistance tests for non-loadbearing elements - Part 1: Walls. Available at: https://standards.iteh.ai/catalog/standards/cen/bea6cc6b-69a7-4281-b2a4-d43b2c4f84dc/en-1364-1-2015?srsltid=AfmBOoqF4Zlvch24inwBta7P7FrdXchQZIkDS4XtfncRBtCvsXe0HPs4
17. Bula, S. S., Boiko, R. O. (2014). Pat. No. 93911 UA. Pich dlia vohnevykh vyprobuvan budivelnykh konstruktsiy ta teplofizychnykh vyprobuvan materialiv. No. u201403476; declareted: 04.04.2014; published: 27.10.2014, Bul. No. 20. Available at: https://sis.nipo.gov.ua/uk/search/detail/659768/
18. ISO 834-1:1999. Fire-resistance tests - Elements of building construction - Part 1: General requirements. Available at: https://www.iso.org/standard/2576.html
19. Incropera, F. P., DeWitt, D. P., Bergman, T. L., Lavine, A. S. (2007). Fundamentals of Heat and Mass Transfer. John Wiley & Sons. Available at: https://ostad.nit.ac.ir/payaidea/ospic/file8487.pdf
20. QuickField. Available at: https://quickfield.com/
21. QuickField. Version 6.6 User's Guide. Available at: https://quickfield.com/downloads/quickfield_manual.pdf
22. Terzic, A., Stojanovic, J., Andric, L., Milicic, L., Radojevic, Z. (2020). Performances of vermiculite and perlite based thermal insulation lightweight concretes. Science of Sintering, 52 (2), 149–162. https://doi.org/10.2298/sos2002149t
23. Sandaka, G., Al-Karawi, J., Specht, E., Silva, M. (2017). Thermophysical properties of lime as a function of origin (Part 4): Thermal conductivity. ZKG International, 70 (3), 36–41. Available at: https://www.zkg.de/en/artikel/zkg_Thermophysical_properties_of_lime_as_a_function_of_origin_Part_4-2772549.html
24. Table of emissivity of various surfaces. Available at: https://www.transmetra.ch/images/transmetra_pdf/publikationen_literatur/pyrometrie-thermografie/emissivity_table.pdf
25. EN 1363-1:2020. Fire resistance tests - Part 1: General requirements. Available at: https://standards.iteh.ai/catalog/standards/cen/243adbdc-e0e0-43ac-a801-22c8e91e7f3c/en-1363-1-2020?srsltid=AfmBOoobqrBIphw5GPrTfIPHaltsdw-iLdsKQy4aTGWV1zyL_CDygVut